Synergistic center-surround receptive field model of monkey H1 horizontal cells

Orin S. Packer

Department of Biological Structure,
University of Washington, Seattle, WA, USA

Dennis M. Dacey

Department of Biological Structure and
National Primate Research Center,
University of Washington, Seattle, WA, USA

Horizontal cells typical of the vertebrate retina are strongly coupled by gap junctions. The resulting horizontal cell network has extremely large receptive fields that extend well beyond the boundaries of a single dendritic tree. This network has been modeled as a syncytium of cytoplasm bounded by cell membrane (Naka & Rushton, 1967, Lamb, 1976). Horizontal cells in the primate retina are also coupled by gap junctions, but their receptive fields are relatively small and in some cases may approximate the span of the dendritic tree of an individual cell (Packer & Dacey, 2002). The receptive field of the macaque H1 horizontal cell type has been modeled as the sum of two spatial components: a strong but small diameter excitatory center, and a weak but broad excitatory surround. Here we explore the hypothesis that the receptive field center of H1 cells derives from direct cone synaptic input and that the synergistic surround derives from gap-junctional coupling among H1 cell neighbors. We measured the receptive field structure of H1 cells in the presence of carbenoxolone, a gap junction blocker, to determine the effects of uncoupling center and surround components and compared these data to a neural simulation of the H1 network in which gap-junctional conductance could be manipulated. Carbenoxolone reduced the surround component and eliminated irregularities in spatial structure thought to be associated with the surround. The effects of carbenoxolone could be mimicked by manipulating gap-junctional conductance in an H1 cell network simulation. These results provide strong support for the two-component model of H1 receptive field structure.

In addition, carbenoxolone eliminated a slow depolarization following light onset thought to be mediated by cone–H1 feedback (Kamermans & Spekreijse, 1999). Low concentrations of cobalt, a calcium channel blocker that spares gap junctions, had an effect similar to that of carbenoxolone but did not affect receptive field structure. These results are consistent with a calcium-mediated mechanism of feedback from H1 cells to cones that is independent of the synergistic two-component model of receptive field organization.

Keywords: carbenoxolone, color opponent, feedback, H1 horizontal cell, primate retina, receptive field, two-component model

Introduction

In most vertebrates, retinal horizontal cells (Dacey et al., 2000; Mangel, 1991; McMahon, Packer, & Dacey, 2004; Naka & Nye, 1971; Naka & Witkovsky, 1972; Packer & Dacey, 2002; Verweij, Hornstein, & Schnapf, 2003) form a network in which large gap junctions mediate strong electrical coupling among horizontal cell dendrites (Kaneko, 1971; Lamb, 1976; Lankheet, Prickaerts, & van de Grind, 1992; Naka & Rushton, 1967; Tomita, 1965; Witkovsky, Owen, & Woodworth, 1983; Yamada & Ishikawa, 1965). This strong coupling results in large horizontal cell receptive fields (Bloomfild, Xin, & Persky, 1995; Mills & Massey, 1994; Tornqvist, Yang, & Dowling, 1988) whose sensitivity falls smoothly as an exponential function of distance from the point of stimulation. Horizontal cell coupling is so strong that the network can be simplified to a thin sheet of cytoplasm of infinite extent bounded by cell membrane (Lamb, 1976; Naka & Rushton, 1967). One function of this coupled network is, via feedback to photoreceptors, to contribute to the creation of the inhibitory receptive field surround of inner retinal neurons.

In primates, by contrast, the anatomical and physiological organizations of horizontal cells are more complex, likely due to the existence of the fovea. The high visual acuity of the fovea is mediated by small ganglion cell receptive fields that in turn require high cone, bipolar, and ganglion cell density and small cell size. Complementary morphological (Wässle, Boycott, & Rohrenbeck, 1989; Wässle et al., 2000) gradients are present in horizontal cells (Figures 1A–C). Foveal H1 horizontal cells, the most common type of primate horizontal cell, have small dendritic arbors (16 μm in diameter) that are densely packed (25,000 cells/mm^2) but overlap only a few of their neighbors (~3). H1 cells in peripheral retina, a region of

doi: 10.1167/5.11.9 Received August 9, 2005; published December 28, 2005 ISSN 1534-7362

reduced resolution, have lower density (1,000 cells/mm^2), larger dendritic arbors (160 μm in diameter), and high dendritic overlap (~30), a pattern more typical of other mammals.

H1 cells show a corresponding central to peripheral gradient of receptive field diameter (see Figure 1B, open circles, solid line). Central H1 receptive fields are small (~120 μm in diameter at 4 mm eccentricity), whereas peripheral receptive fields are larger (~310 μm diameter at 11 mm eccentricity) and extend beyond the dendritic tree. However, H1 receptive fields are poorly fit by the classic infinite sheet model (Naka & Rushton, 1967) that predicts that sensitivity profiles will be well fit by a single exponential function. Instead, the sensitivity profile of most H1 receptive fields takes the form of a narrow peak superimposed on a broad skirt and must be fit by a sum of two exponential components (Figure 1D).

We previously hypothesized (Packer & Dacey, 2002) that the two-part receptive field of H1 horizontal cells is the sum of a strong but small diameter "center" mediated by direct cone synaptic input and a broad but weaker "surround" mediated by coupling. This synergistic "center-surround" receptive field model suggests a mechanism by which H1 cells can adjust the strengths of the two parts of the receptive field as a function of eccentricity to optimize their contribution to ganglion cell surrounds. In central retina, a small minimally coupled dendritic tree can likely form a receptive field small enough to mediate a midget ganglion cell surround; whereas in peripheral retina, a large and extensively coupled dendritic tree can form a large receptive field consistent with large peripheral ganglion cell surrounds. The small H1 receptive field of central retina, which indiscriminately contacts a handful of randomly arranged L and M cones, also guarantees that a small number of H1 receptive fields will contact only L or M cones, providing a potential mechanism for sharpening red/green spectral opponency (Dacey & Packer, 2003).

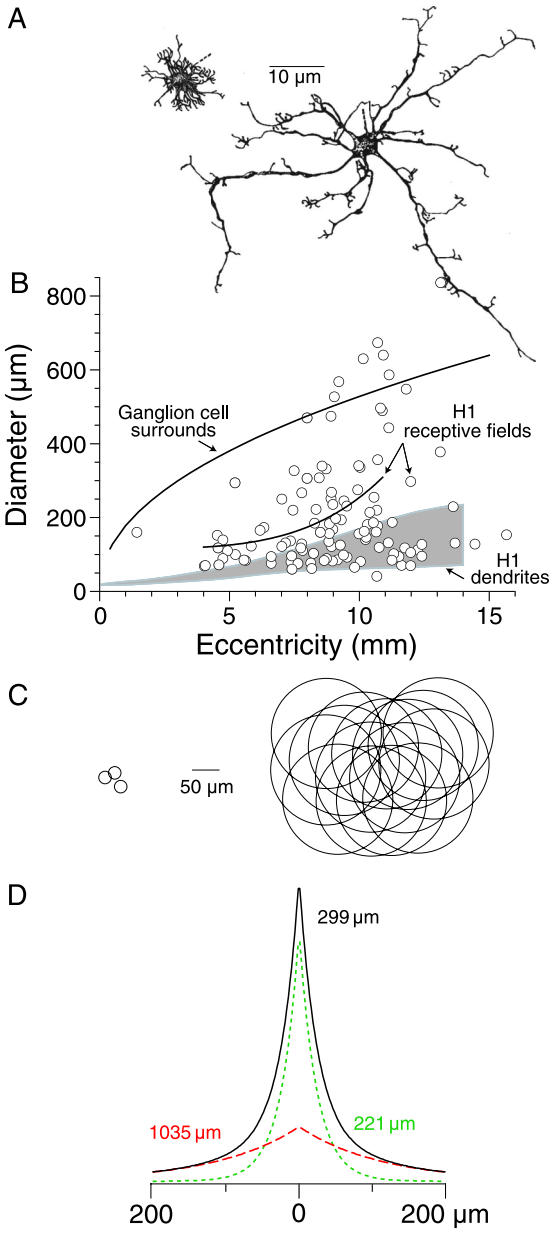

Figure 1. An overview of the anatomy and physiology of primate H1 horizontal cells. (A) Two drawings of H1 dendritic trees that illustrate the change in morphology as eccentricity increases from 2.9 mm (left) to 9.7 mm (right). (B) The plot illustrates changes in dendritic tree and receptive field diameters (μm) as a function of eccentricity (mm). The gray shaded area, which encloses the anatomical measurements of H1 dendritic tree diameter calculated from Wässle et al. (1989), shows the increase in diameter as a function of eccentricity. The open circles, physiological measurements of H1 receptive field diameter from Packer and Dacey (2002), show the increase in receptive field diameter as a function of eccentricity. The lower curve is fit to the H1 receptive field data using the equation $y = y_0 + Ax^t$, where $y_0 = 116.15$, $A = 0.01857$, and $t = 3.8718$. The fit was limited to data up to 11 mm of eccentricity because at greater eccentricities the number of cells measured was too small to capture the full range of receptive field sizes. Receptive field diameter was measured at 0.1 of peak value. For comparison with the H1 data, the upper curve, from Croner and Kaplan (1995), shows the increase in the size of ganglion cell surrounds as a function of eccentricity. (C) An illustration of the increase in the degree of overlap among adjacent dendritic trees from a value of ~3 in the fovea (left) to a value of ~30 in far periphery (right) (Packer & Dacey, 2002). (D) An example of an H1 cell whose receptive field was well fit by a sum of two exponentials (solid black, diameter = 299 μm), a tall narrow "center" (dotted green, diameter = 221 μm), and a broad shallow "surround" (dashed red, diameter = 1035 μm). The ordinate is linear amplitude.

The purpose of this paper was to test several predictions of the two-part receptive field hypothesis using computational, physiological, and pharmacological techniques. Our hypothesis predicts that the sensitivity profile of the cone synaptic component measured in isolation would have a diameter similar to that of the H1 dendritic field sampling the cone mosaic and that response strength would decline smoothly with increasing distance from the point of stimulation. The hypothesis also predicts that the coupled component measured in isolation would have a very broad receptive field with low sensitivity whose diameter was larger than a single H1 dendritic field. To test these and other predictions, we used a compartmental model of the cone–H1 horizontal cell network (Smith, 1992, 1995) to explore the responses to drifting sinusoidal gratings of an H1 cell whose cone synapses were disconnected. Finally, the hypothesis predicts that the range of shapes seen in the physiological data might result from receptive fields that are dominated by cone synaptic input but have coupled inputs of varying strength. Cells with less coupling would have the small diameter receptive fields and smooth spatial tuning curves characteristic of the cone synaptic input, whereas cells with more coupling would have larger receptive fields. To test this prediction, we varied the gap junction conductance of a compartmental model of the cone–H1 horizontal cell network. We also attempted to measure the effects of reduced gap-junctional coupling directly by recording from H1 cells in an *in vitro* preparation of the retina (Dacey & Lee, 1994; Dacey, Lee, Stafford, Pokorny, & Smith, 1996) during application of the gap junction blocker, carbenoxolone (Davidson & Baumgarten, 1988; Guan, Wilson, Schlender, & Ruch, 1996; Osborne & Williams, 1996; Vaney, Nelson, & Pow, 1998). Finally, we explored the contribution of H1 cells to center-surround receptive field organization by measuring the effects of low concentrations of the Ca^{++} channel blocker, cobalt, previously hypothesized to selectively block feedback from horizontal cells to cones (Kamermans et al., 2001; McMahon et al., 2004; Thoreson & Burkhardt, 1990; Vigh & Witkovsky, 1999).

Taken together, our results strongly support the synergistic center-surround model of the H1 receptive field. Isolating the cone synaptic component with carbenoxolone reduced the receptive field diameter and smoothed the spatial tuning curves of H1 cells hypothesized to have a significant coupled input. Computationally isolating the coupled component confirmed its relatively large receptive field diameter. Varying the coupling strength of the compartmental model and the application of carbenoxolone both reproduced the range of shapes of H1 spatial tuning curves measured physiologically (Packer & Dacey, 2002). Both carbenoxolone and cobalt eliminated a slow depolarization following light onset thought to be mediated by cone–H1 feedback (Kamermans et al., 2001).

Methods

Compartmental model of the cone–H1 network

We simulated the spatial receptive field organization of the cone–H1 horizontal cell network using a compartmental model (Smith, 1995) that divided the neural network into a series of connected compartments, each of which is a small volume of cytoplasm bounded by membrane whose response to electrical stimulation can be described by a relatively simple set of equations. The voltage response of the simulated network to stimulation is calculated by applying these equations repetitively to each compartment at a series of time steps. The compartmental model was created using NeuronC, a neural circuit simulation language (Smith, 1992).

The initial step in modeling the cone–H1 network was defining the neural circuitry (Figure 2). The positions of 2,040 cones were digitized from a patch of cone mosaic imaged using Nomarski optics. The positions of 65 H1 cells were digitized from a patch of coupled H1 cells filled with biocytin. The mosaic was revealed by iontophoretically filling a single cell with biocytin, allowing it to pass through gap junctions into neighboring cells, and using horseradish peroxidase histochemistry to convert the biocytin into a dark reaction product. Models of cones and H1 horizontal cells were created by connecting spheres and cables with appropriate electrical properties. The physiological parameters of the model were set to measured values found in the literature and summarized in Table 1. We used the parameters found in Smith (1995) unless we determined that the primate cone–H1 network required a different value. Each cone (Figure 3A) was modeled as a transducer connected to outer and inner segments represented by spheres, a cone axon represented by a cable and a cone pedicle represented by another sphere. Each horizontal cell (Figure 3B) was modeled as a soma represented by a sphere and a set of dendrites, each represented by a cable. Model cones and H1 cells were connected into a network with models of synapses and gap junctions. Each horizontal cell was connected to each cone located within its dendritic field (Figure 2, dark circle) by a dendrite. Each cone contacted the spine of the horizontal cell dendrite with an excitatory conventional synapse and a reciprocal inhibitory synapse. Horizontal cells were connected to their nearest neighbors with resistive gap junctions.

Our model contained simplifications designed to ease computation while preserving the essential spatial properties of the cone–H1 network. First, all cones were assigned the L cone spectral sensitivity because both L and M cone inputs are summed by H1 cells (Dacey et al., 1996), contribute to luminance responses, and have highly overlapping spectral

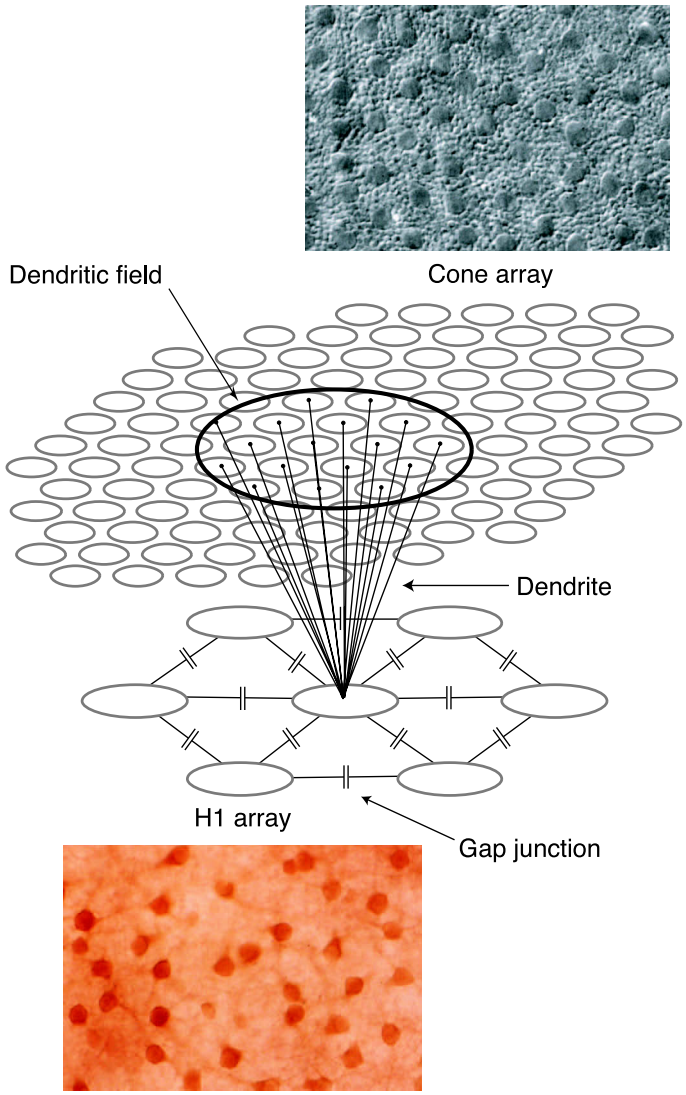

Figure 2. A schematic diagram of the neural circuit model used to simulate the response of the cone–H1 network. A layer of photoreceptors is interconnected with a layer of H1 horizontal cells by conventional synapses and gap junctions. Although shown in the schematic as crystalline triangular arrays, the positions of the somas of the cell mosaics were actually measured from patches of peripheral retina. Cone position was digitized from an image made using Nomarski optics. Horizontal cell position was digitized from a patch of horizontal cells filled by iontophoresis of biocytin. Each H1 cell was connected by gap junctions to all of its nearest neighbors. Each H1 cell was connected by dendrites to all of the cones lying above the 120-μm diameter dendritic field. For clarity, these connections are shown only for a single H1 cell. See Table 1 for other model parameters.

sensitivities. H1 cells lack S cone input (Dacey et al., 1996). Second, we omitted coupling among cones because, at least in the fovea, it is unlikely to be strong enough to reduce the resolution of the mosaic (Hsu, Smith, Buchsbaum, & Sterling, 2000). Third, we moved horizontal cell coupling from the dendrites to the somas. Fourth, we modeled horizontal cell dendrites as unbranched cables between the H1 soma and a cone pedicle. The last two simplifications eliminated the need to make complicated models of H1 dendritic trees while preserving the radial pattern and strength of coupled inputs. We also substantially simplified the cone–H1 synaptic circuitry, for example, by leaving out the calcium-activated chloride current, because the details are unlikely to affect the spatial organization of the H1 receptive field. Finally, the model is passive and includes no voltage-dependent currents.

NeuronC converted the neural circuit representing the cone–H1 network into a series of compartments. The compartmental model was stimulated with a 5-Hz drifting sine wave grating by having cone transducers apply a time-varying voltage modeled after that of real cone responses to those compartments of the model representing cone outer segments. This signal passively propagated through the compartments. The output of the model was the voltage response of the compartment representing the central soma of the horizontal cell mosaic calculated for each time step. For each of a series of spatial frequencies, we calculated the fundamental response to the grating at the 5-Hz drift frequency using a digital Fourier transform. A spatial tuning curve was constructed by plotting response amplitude as a function of spatial frequency.

Tissue preparation

Macaque monkey (*Macaca nemestrina, Macaca fascicularis*) and baboon (*Papio cynocephalus anubis*) retinas were obtained through the tissue program of the

Model cone	
Aperture diameter	8 μm
Inner segment length	5 μm
Membrane resistance	20,000 Ω
Resting membrane potential	−37.7 mV
Terminal resting membrane potential	−37.7 mV
Model H1	
Soma diameter	15 μm
Soma resting membrane potential	−45 mV
Dendritic field diameter	120 μm
Dendrite tip resting membrane potential	−41 mV
Dendrite diameter	2 μm
Network	
No. of cones	2,040
No. of H1 cells	65
H1 to H1 gap junction resistance	1.00E−07 Ω
Stimulus	
Photon flux irradiance	10,000 quanta/s/μm^2
Drift rate	5 Hz
Grating contrast	100%

Table 1. Parameters of the cone–H1 network model.

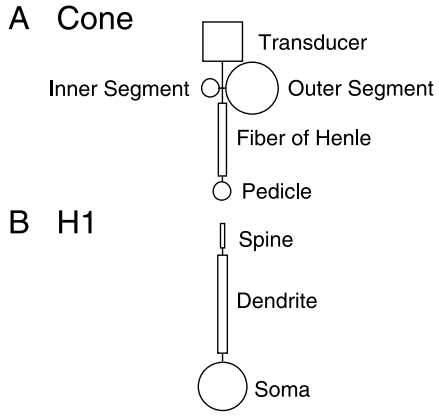

Figure 3. A schematic diagram of the model circuitry of cones and horizontal cells. (A) The model cone consists of a transducer connected to inner and outer segments and to the cone axon that ends in a cone pedicle. When stimulated by light, the transducer produces a voltage response modeled after the response of real cones. This response passively travels into the spheres representing the inner and outer segments, down the cable representing the cone axon and into the sphere representing the cone pedicle. (B) The model H1 cell consists of a sphere representing the soma and any number of cables, each of which represents a dendrite. At the end of each dendrite is a short cable representing a synaptic spine. The electrical and geometrical parameters of the cells are listed in Table 1.

National Primate Research Center at the University of Washington. In brief (see Dacey & Lee, 1994; Dacey et al., 1996), the retina, choroid, and pigment epithelium were dissected as a unit from the vitreous and sclera and placed in oxygenated Ames medium (Sigma). They were then mounted vitreal side up in a superfusion chamber mounted on a microscope stage. H1 horizontal cell nuclei were stained with 4,6 diamidino-2-phenylindole (DAPI) (10 μM) and identified under the microscope by their depth in the retina and the large size, granularity and semiregular arrangement of their somas. Targeted nuclei were penetrated with glass microelectrodes filled with 3% biocytin and 2% pyranine in 1 M KCl or 1 M K acetate. Electrode impedance exceeded 200 MΩ. Iontophoresis of pyranine allowed confirmation of cell identity by revealing the dendritic morphology. Horizontal cells were imaged *in vitro* during the experiment and later from the mounted retina using a CCD camera attached to the microscope. Some cells were filled with biocytin (Molecular Probes) by iontophoresis through the recording electrode; 0.1–0.5 nA for 10–30 min). This tracer easily crosses gap junctions between H1 dendrites and diffuses through a patch of H1 cells. At the end of the experiment, the retina was dissected from the pigment epithelium and choroid, fixed in phosphate buffered 4% paraformaldehyde for 2 hr, and stored in phosphate buffer (pH 7.4). Standard horseradish peroxidase histochemistry converted the biocytin into a black reaction product. The retina was then mounted on a slide using a solution of polyvinyl alcohol and glycerol. H1 cells stained using the Golgi method were photographed from retinas donated to the lab by R.W. Rodieck.

Stimuli

Once a stable recording was established, stimuli were created using a digital light projector (DLP) (Packer et al., 2001) and imaged on the retina through the camera port of the microscope. Stimuli were modulated around a mean light level of ~1,000 trolands to hold the light adapted state of the retina constant at a light level at which rod responses were largely saturated.

The receptive field center of each cell was found by moving a small flickering (2 Hz) spot of light to the position of maximum response and making this position the center of subsequent stimulation. Stimuli were optimized to evoke luminance responses by setting all three chromatic channels of the stimulator to the same proportion of maximum light output. Stimulus contrast was set to 100%, consistent with previous findings (Packer & Dacey, 2002; Smith, Pokorny, Lee, & Dacey, 2001) that high contrast stimuli elicit large responses without driving the cells out of their linear response range. The resulting stimuli modulated from black to white. H1 horizontal cell receptive fields were stimulated with flashing spots and drifting sinusoidal gratings. Responses to flashing spots were elicited with a spot 2 mm in diameter that extended well past the receptive field of the cell. Spot intensity was square wave modulated at a frequency of 2.44 Hz. Spatial receptive field structure was characterized by drifting sinusoidal gratings across the retina at a fixed temporal frequency of either 2, 4, or 10 Hz and plotting response amplitude as a function of spatial frequency.

Data acquisition

The intracellular voltage response of the cell penetrated by the electrode was amplified (Axon Instruments, Axoprobe-1A), digitized (National Instruments, NBIO16 installed in a Macintosh computer) at a sampling rate of up to 10 kHz, and averaged over several stimulus cycles. A digital Fourier transform calculated the amplitude and phase of the response at the temporal frequency of stimulus modulation.

Pharmacology

Pharmacological agents were added to the Ames medium superfusing the retina during recording. We tested the effects of 100 μM carbenoxolone (Sigma C4790), thought to block retinal gap junctions (Davidson & Baumgarten, 1988; Guan et al., 1996; Osborne & Williams, 1996; Vaney

et al., 1998), on H1 cell receptive field structure. Other agents, including retinoic acid and dopamine (Vaney et al., 1998; Weiler, Pottek, He, & Vaney, 2000), also block gap junctions, but we chose carbenoxolone because it is water soluble and because its actions were thought to be more specific to gap junctions than other agents (although see also Vessey et al., 2004). We also tested the effects of 100 μM cobalt (Aldrich 232696) on H1 responses. Both drugs have been found to attenuate H1 horizontal cell feedback onto cones, bipolar cells, and ganglion cells (Kamermans et al., 2001; McMahon et al., 2004; Thoreson & Burkhardt, 1990; Vigh & Witkovsky, 1999).

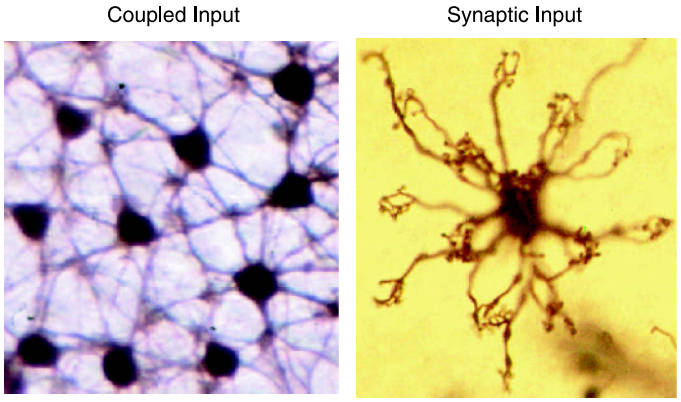

Figure 4. The anatomy of cone input to H1 cells of the primate retina. On the left is a patch of the horizontal cell network. Biocytin (3%), injected by iontophoresis into a single soma, passed through the gap junctions among H1 dendrites filling the entire network. Horseradish peroxidase histochemistry converted the tracer to a black reaction product. On the right is an image of an H1 cell stained using the Golgi method showing the synaptic terminals at the tips of the dendrites. Each cluster of terminals makes multiple synapses with a single cone.

Results

H1 horizontal cells have the anatomical characteristics required to support the two-component hypothesis of receptive field organization

Synapses between cone pedicles and synaptic terminals located at the ends of H1 cell dendrites (Figure 4, right) form the anatomical basis for a direct synaptic input. Each dendritic branch ends in a cluster of synaptic terminals that make multiple contacts with a single cone pedicle. A highly overlapping network of H1 dendrites (Figure 4, left) forms the anatomical substrate for a coupled input. When biocytin is injected into a single H1 cell, it diffuses into the dendritic tree and through gap junctions between crossing dendrites and is revealed by subsequent HRP histochemistry.

Peripheral H1 horizontal cell receptive fields vary substantially in size and organization at any given retinal eccentricity

To better understand the contributions of the synaptic and coupled inputs, we first measured overall H1 receptive field organization by drifting a series of sinusoidal gratings of increasing spatial frequency across the receptive field and plotted response amplitude as a function of spatial frequency. Additional examples including illustrations of individual H1 responses to stimuli as well as extensive controls have been previously published (Packer & Dacey, 2002). In brief, these spatial tuning curves confirmed that the majority of cells had relatively broad spatial tuning curves, corresponding to relatively small receptive fields, whose response declined smoothly with increasing spatial frequency (Figure 5, top curve). These tuning curves were well fit by a sum of two exponential functions except at the highest spatial frequencies. In light of the two-component hypothesis, these results suggest that most receptive fields are dominated by synaptic input but also have a substantial coupled input. Other cells had tuning curves with a shoulder at intermediate spatial frequencies (Figure 5, middle two curves). The response amplitudes of these tuning curves rolled off more quickly, corresponding to cells with larger receptive fields. Finally, the responses of some cells not only rolled off quickly but also had a prominent notch at intermediate spatial frequencies (Figure 5, bottom curve). Only the lowest frequencies of these tuning curves could be fit with an exponential function. These cells likely have a stronger coupled input whose addition to the synaptic input increases receptive field size and emphasizes spatial interactions arriving from the H1 network.

A compartmental model of the cone–H1 network predicts both the shape and the irregularities of measured H1 spatial tuning curves

Initially, we evaluated the infinite sheet model used to predict the horizontal cell receptive field properties of other vertebrate retinas (Lamb, 1976; Naka & Rushton, 1967) but found that its prediction of uniformly large receptive fields across the retina did not match the robust peripheral to central decreases of diameter measured in dendritic arbors and receptive fields (Packer & Dacey, 2002; Wässle et al., 1989, 2000). Nor did measured receptive field sensitivity decline exponentially as a function of distance from a point of stimulation.

In light of these inconsistencies, we developed an alternative synergistic center-surround description of the

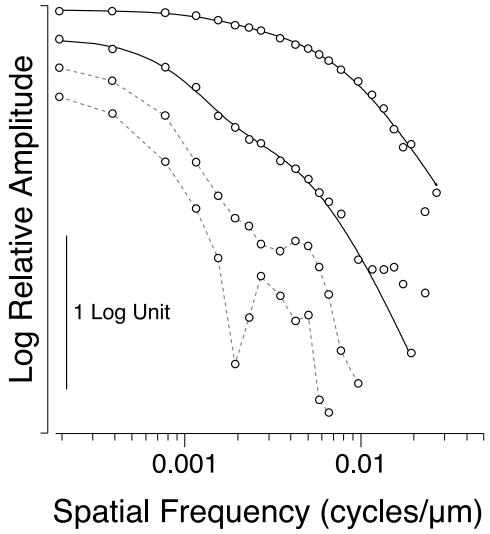

Figure 5. Examples of the range of shapes of H1 cell spatial tuning curves. Each tuning curve was normalized to its peak amplitude. The ordinate is log relative amplitude. The curves have been arbitrarily shifted vertically to make comparison easier. The scale bar shows a 1 log unit change in response amplitude. Top curve: An example of a cell with a smooth spatial tuning curve (open circles) that can be fit by a sum of two exponential functions (solid line). Middle curves: Examples of cells that have an inflection at moderate spatial frequencies. Slightly inflected curves, but not more deeply inflected ones, can be fit with a sum of two exponentials (solid line). Bottom curve: An example of a cell with a deep notch at intermediate spatial frequency. The data points of tuning curves that cannot be fit by a sum of exponentials are connected with a dashed line.

H1 horizontal cell network by creating a compartmental model (see Methods) of the cone–H1 circuitry that included both synaptic and coupled inputs to H1 cells. We stimulated the model with 5 Hz drifting sine wave gratings of a range of spatial frequencies, calculated the voltage response of the central H1 cell, and plotted a model spatial tuning curve. This curve (Figure 6A) had a response amplitude that declined smoothly from a peak at the lowest spatial frequency until interrupted by a deep notch at an intermediate spatial frequency. In short, its characteristics were similar to those cells that we previously interpreted as having relatively strong coupled input (Figure 5, bottom) and suggests that a two-component model of H1 receptive field organization with an appropriate degree of H1–H1 coupling can account for even the unusual features of measured spatial tuning curves.

The compartmental model of the cone–H1 network also predicts the spatial properties of isolated synaptic and coupled inputs

In light of the success of the model at predicting the spatial tuning curves of H1 cells receiving mixed

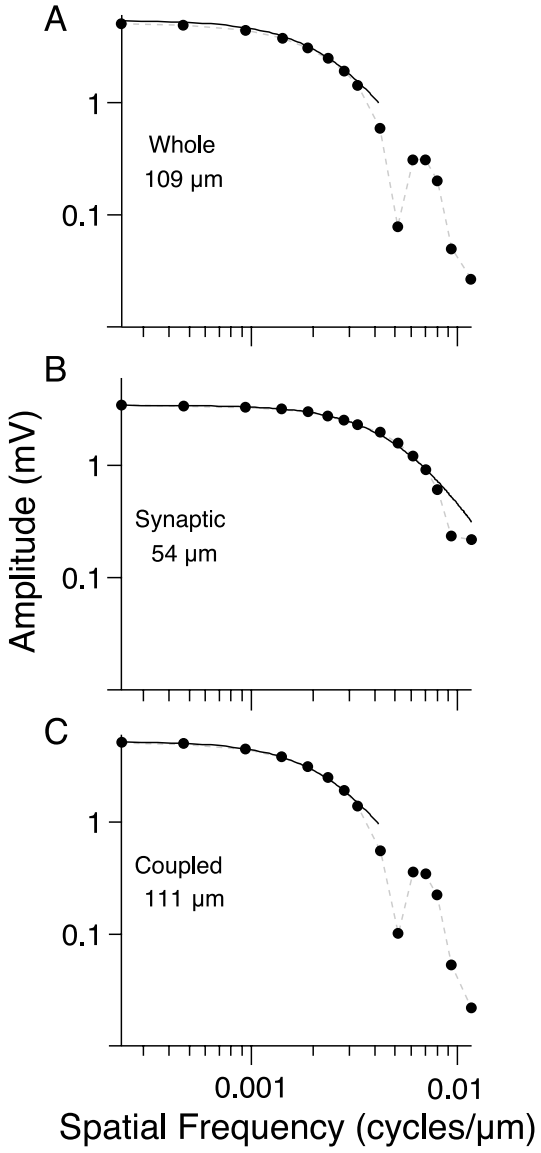

Figure 6. The model spatial tuning curves (filled circles connected by dashed line) and best-fitting sum of two exponentials (solid curves) of the central H1 cell of the cone–H1 network model when stimulated with 5 Hz drifting sinusoidal luminance gratings at a series of spatial frequencies. (A) The spatial tuning curve of the central H1 cell getting both direct synaptic input from cones and coupled input arriving via gap junctions from neighboring H1 cells. The receptive field diameter of the best-fitting sum of two exponential functions was 109 μm. (B) The spatial tuning curve of the central H1 cell after disconnecting the coupled input by increasing gap junction resistance to infinity. Best-fitting receptive field diameter was 54 μm. (C) The spatial tuning curve of the central H1 cell after disconnecting the direct synaptic inputs to that cell alone. Best-fitting receptive field diameter was 111 μm. The model responses to full-field square wave temporal modulation look like the responses of H1 cells with reduced onset and offset transients. There is no slow depolarization because we did not model a detailed cone–H1 synapse. When the gap junctions are opened, the shape remains similar but the amplitude decreases modestly.

synaptic and coupled cone input, we next modeled the receptive field properties of each of the two components in isolation.

The model response to cone synaptic input alone was simulated by disconnecting the gap junctions between neighboring H1 cells. Before the coupled input was disconnected (Figure 6A), amplitude stayed high until ~0.002 cycles/μm before beginning a rapid decline into a notch at ~0.005 cycles/μm. When the coupled input was disconnected (Figure 6B), amplitude stayed high until ~0.005 cycles/μm. This increase in the spatial frequency at which the tuning curve begins to roll off sharply indicates a decrease in receptive field diameter. Without H1 coupling (Figure 6B), receptive field diameter estimated from the fits of the sum of exponentials model decreased from 109 to 54 μm. In addition to the decrease in receptive field diameter, the notch at ~0.005 cycles/μm was eliminated, strongly suggesting that this irregularity was a property of the now eliminated coupled input. These results are also consistent with the predicted receptive field properties of the synaptic input to the two-component hypothesis.

The model response to the coupled input alone was simulated by disconnecting the cone synapses contacting the recorded H1 cell (Figure 6C). Under these conditions, the response was not substantially different than the response of the cell with all inputs intact (Figure 6A). Both the receptive field diameter estimated from model fits (55 vs. 54 μm) and the shape of the tuning curve of the isolated coupled input remained very similar to those of the composite response. Response amplitude was also similar. These results are consistent with the predicted receptive field properties of the coupled component of the two-component hypothesis and suggest that the diameter of the H1 receptive field is largely determined by the coupled input and that the coupled input is the source of irregularities in the spatial tuning curves. In addition, the shift from a narrow and irregular tuning curve to a broader smoother one that was produced by reducing coupling strength mimics the range of measured receptive field tuning curves. This suggests that the variability in the tuning curves of peripheral H1 cells measured physiologically can be explained by variations in physiological coupling strength from cell to cell.

The effects of carbenoxolone and cobalt on the physiological responses of H1 horizontal cells to flashing spots

As previously reported (Dacey et al., 1996; Dacheux & Raviola, 1990; Packer & Dacey, 2002; Smith et al., 2001), H1 cells had a stereotypical response to a large white spot that filled the receptive field and was square wave modulated at a low temporal frequency (2.44 Hz). Cells rapidly hyperpolarized at light onset and then slowly depolarized back to a resting potential dependent on the new light level (Figure 7, Before). When the light was turned off, the reverse happened. Cells depolarized rapidly and then slowly hyperpolarized back to their resting potential in the dark.

About 2 min after 100 μM carbenoxolone began to superfuse the retina, the slow depolarization following light onset was abolished (Figure 7, Cells 1–2, Carbenoxolone). The shape of the response following light offset was not noticeably changed. As soon as the slow depolarization was abolished, we ended drug superfusion and began recording light responses. Typically, it was possible to make several measurements of receptive field characteristics before the cell began to hyperpolarize and a substantial loss of responsiveness was noticed. By ending superfusion as soon as the cell began responding to the drug, we could often prevent any substantial loss of responsiveness. We made our measurements before the light response dropped by more than a factor of two. Several minutes after the drug induced loss of the slow depolarization, there was a reduction in response amplitude ($n = 30$) that averaged

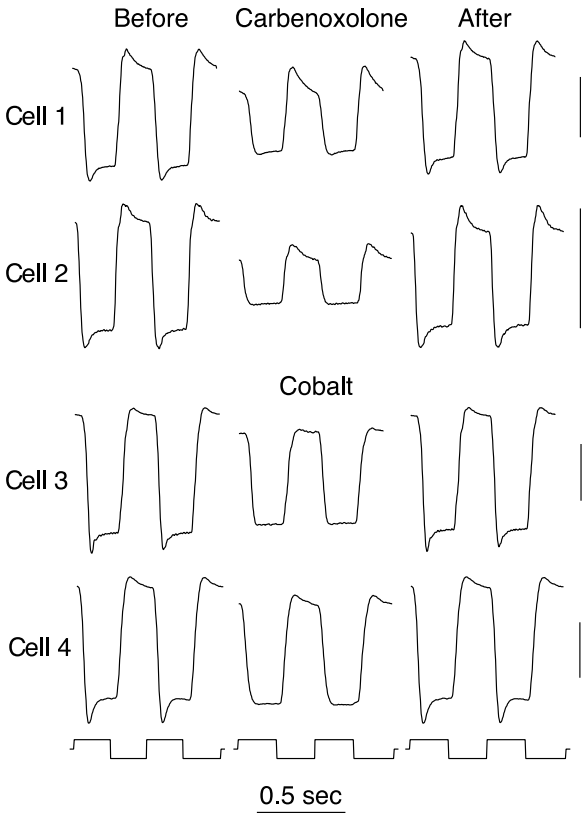

Figure 7. The responses of 4 H1 cells to a 2.44-Hz flashing spot that filled the receptive field. Each row shows two response cycles of a single cell before, during, and after superfusion with 100 μM carbenoxolone (Cells 1–2) or 100 μM cobalt (Cells 3–4). Each response is the average of three stimulus presentations. The vertical scale bars on the right indicate 10 mV of amplitude. The timing of light onset and offset is shown at the bottom.

a factor of ~2, although the extent of the reduction varied substantially. Simultaneously, the resting potential hyperpolarized by 20–30 mV. Light responses were often abolished completely by continued superfusion or by concentrations exceeding 100 μM. Most cells recovered their slow depolarization and original response amplitude ~30 min after superfusion ended (Figure 7, Cells 1–2, After).

H1 cells ($n = 8$) responded to 100 μM cobalt in way similar to their response to carbenoxolone (Figure 7, Cells 3–4). As cobalt took effect, cells hyperpolarized slightly and the depolarization following light onset was abolished. Some cells also lost response amplitude with continued superfusion although both amplitude loss and hyperpolarization were less pronounced for cobalt than carbenoxolone. As with carbenoxolone, we began recording as soon as the slow depolarization disappeared to minimize any secondary effects the drug was having on the retina. Most cells recovered their original responses within several minutes after drug superfusion ended.

The elimination of the slow depolarization in the response of H1 cells to a flashing spot after the application of carbenoxolone and cobalt was very similar to the effects of these drugs on teleost horizontal cells (Kamermans et al., 2001). These authors hypothesized that the slow depolarization is due to feedback from the horizontal cell to the cone photoreceptor. According to this hypothesis, cobalt blocks calcium-dependent feedback whereas carbenoxolone blocks hemichannels on horizontal cell dendrites in the synaptic cleft between horizontal cell and cone pedicle. Our results are consistent with this hypothesis. The responses of H1 horizontal cells to square wave stimulation have the same slow depolarization. The slow depolarization is similarly eliminated by superfusion of carbenoxolone or cobalt.

Finally, we used the suppression of the slow depolarization by carbenoxolone and cobalt as an assay to indicate the presence of the drugs on the retina during further measurements of receptive field organization.

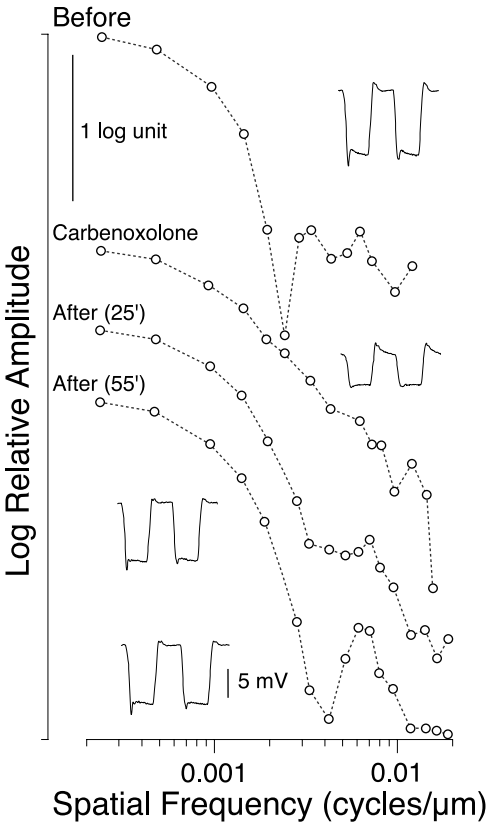

Figure 8. The spatial tuning curves (open circles) and spot responses of an H1 cell before, during, and after superfusion of 100 μM carbenoxolone. Each tuning curve was normalized to its maximum value for easier comparison of curve shapes. The ordinate is log relative amplitude. Each curve is arbitrarily shifted vertically. The upper left scale bar shows a 1 log unit change in response amplitude. Relative tuning curve amplitudes can be estimated by comparing the unnormalized amplitudes of the spot responses near each tuning curve. The 5-mV scale bar applies to all of the spot responses. Top curve: Normalized spatial tuning curve and response to a 2.44-Hz flashing white full-field collected before drug application. Second curve from top: The normalized tuning curve and spot responses ~5 min after application of carbenoxolone. The slow depolarization had just vanished. Bottom two curves: The normalized spatial tuning curves and spot responses 25 and 55 min after drug superfusion ended.

Carbenoxolone, but not cobalt, reduced H1 receptive field amplitude, diameter, and irregularity

To test the predictions of the model that blocking the coupled input to the H1 cell would reduce receptive field diameter and attenuate irregularities in the spatial tuning curves, we measured the effects of carbenoxolone and cobalt on H1 cell receptive field structure. We previously found (Packer & Dacey, 2002) that the response amplitude of ~20% of H1 cells stimulated with a drifting sinusoidal grating declined rapidly as spatial frequency increased and had additional notches and deflections at mid to high spatial frequencies. The cell shown in Figure 8 is of this type. At the lowest spatial frequencies, the cell responded strongly. Up to spatial frequencies of ~0.002 cycles/deg, the response decreased smoothly (Figure 8, Before) but then becomes irregular at higher spatial frequencies. This cell also had a well-developed slow depolarization following the light onset of a 2.44-Hz white full-field flashing spot (Figure 8, insets). After the application of 100 μM carbenoxolone, the deep notch in the spatial tuning curve at 0.002 cycles/μm disappeared and the rate of response decline as a function of spatial frequency was less than that before the drug was applied (Figure 8, Carbenoxolone).

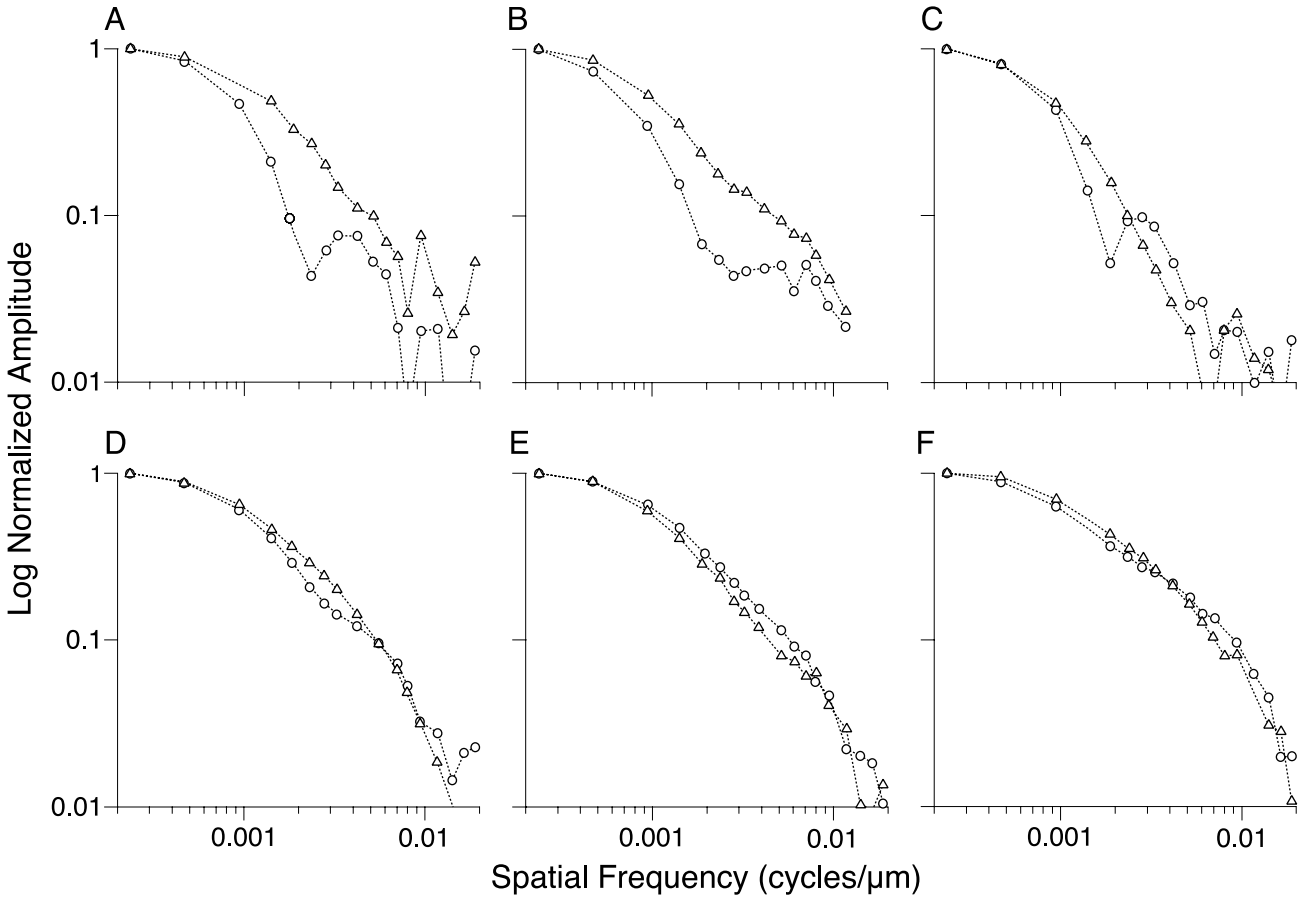

Figure 9. The responses of 6 H1 cells to drifting sinusoidal luminance gratings as a function of spatial frequency before (open circles) and during (open triangles) superfusion of 100 μm carbenoxolone. Each graph represents a different cell. For ease of comparison, each spatial tuning curve was normalized to its peak value. The open circles in each graph are the spatial tuning curves collected before application of carbenoxolone. The spatial tuning curve was collected as soon as possible after carbenoxolone abolished the slow depolarization in the response to a 2.44-Hz white full-field flashing spot. (A–C) Three examples of cells with irregular tuning curves. (D) An example of a cell whose tuning curve had a slight inflection at intermediate spatial frequency. (E–F) Two examples of cells with smooth tuning curves.

This broadening of the spatial tuning curve is equivalent to a decrease in the diameter of the receptive field from a diameter of 286 μm before application to a diameter of 188 μm after application. Twenty-five minutes after carbenoxolone superfusion ended (Figure 8, After (25′)), the deep notch began to reappear as did the slow depolarization in the spot response. Fifty-five minutes after drug superfusion ended (Figure 8, After (55′)), the resting membrane potential (not shown) as well as the amplitude and shape of the tuning curve and spot response had recovered to near their initial values.

We measured the receptive field structure and flashing spot responses of 24 H1 horizontal cells before, during, and when possible after the application of carbenoxolone. As previously reported (Packer & Dacey, 2002), the shapes of the spatial tuning curves ranged from smooth to heavily notched. Figure 9 shows examples of tuning curves that are typical of the range measured. Eight cells had tuning curves with at least one deep notch usually at an intermediate spatial frequency (Figures 9A–C, open circles; also Figure 8), five cells had tuning curves with an inflection at intermediate spatial frequencies (Figure 9D, open circles), and 11 cells had smooth spatial tuning curves (Figures 9E–F, open circles).

The spatial tuning curves of cells with larger receptive fields and irregular spatial tuning curves were more strongly affected by carbenoxolone than cells with smaller receptive fields and smooth spatial tuning curves. Carbenoxolone reduced the depth of notches at intermediate spatial frequencies and reduced the diameter of the receptive field in six of eight cells with the bumpiest tuning curves. In the three examples shown (Figures 9A–C), note the smoother shapes and shallower slopes of the tuning curves during drug application (open triangles) than before drug application (open circles). Carbenoxolone reduced the depth of inflections in all five cells with intermediate

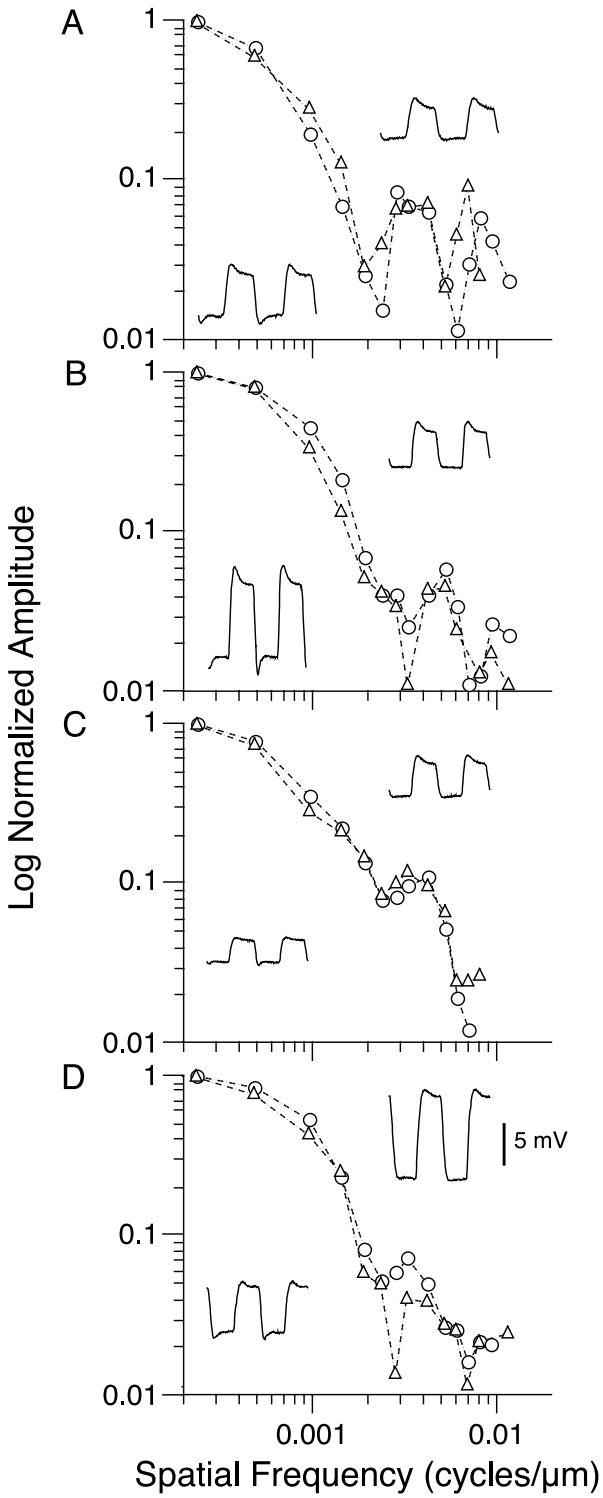

Figure 10. Spatial tuning curves of 4 H1 cells ($n = 6$) to drifting sinusoidal luminance gratings as a function of spatial frequency before (open circles) and after (open triangles) the application of 100 μm cobalt chloride. For ease of comparison, each spatial tuning curve was normalized to its peak value. The lower left and upper right insets in each figure are the responses to a square wave modulated full-field luminance stimulus before and after cobalt application respectively. The 5-mV scale bar applies to all of the inset responses.

spatial tuning curves as shown by the example in Figure 9D but had little effect on any of the 11 cells with smooth spatial tuning curves (Figures 9E–F).

On the other hand, H1 receptive field structure was little affected by the application of 100 μM cobalt chloride (Figure 10). Cells selected for their large receptive fields and irregular spatial tuning curves had notches at intermediate spatial frequencies that were unaffected by the application of cobalt even though there was a robust reduction of the slow depolarization during drug application (Figure 10, insets). Response amplitude during drug superfusion varied as shown by the responses to a full-field flashing spot. The most common change was a reduction in amplitude during superfusion, but a few responses actually increased during superfusion and washout, likely due to an improving electrode seal.

These results are consistent with the predictions of the two-component hypothesis and suggest that carbenoxolone blocks the gap junctions among H1 dendrites. This eliminates the coupled component of the receptive field that reduces receptive field diameter and amplitude and blocks any spatial interactions in the coupled input that contribute to the irregularity of the spatial tuning curve. On the other hand, cobalt does not block H1–H1 gap junctions and therefore has little effect on receptive field properties.

Discussion

Synergistic organization of H1 receptive fields

After finding that the infinite sheet model used to predict the horizontal cell receptive field properties of other vertebrate retinas (Lamb, 1976; Naka & Rushton, 1967) did not accurately predict H1 physiology (Packer & Dacey, 2002), we developed an alternative synergistic center-surround model of the H1 horizontal cell network in which cone synaptic input to the dendritic tree defined the receptive field center and a second input via gap junctions provided an excitatory surround. We are not the first to hypothesize a synergistic receptive field for horizontal cells. Shigematsu and Yamada (1988) showed that the receptive fields of carp luminance horizontal cells were best fit by a synergistic two-component model. However, there are fundamental differences in the origin of the receptive field inputs to the luminance horizontal cells of fish and monkey. In both cases, one component of the receptive field is mediated by coupling among neighboring horizontal cells. In carp horizontal cells, the second component comes from the axon terminal. By contrast, the second component of the primate H1 receptive field is mediated by direct cone synaptic input.

Even the large receptive fields of peripheral H1 cells are dominated by cone synaptic input. The coupled component of the H1 receptive field never achieves the dominance, even in the far periphery, of the strong but small diameter center typical of H1 receptive field sensitivity profiles (Figure 1D).

Nevertheless, the coupled component plays an important role in determining receptive field characteristics. Receptive field diameter appears to be largely determined by the breadth of the coupled input as shown by the minimal change in overall receptive field diameter that results from computationally disconnecting direct cone input (Figure 6C). Although strong, the cone synaptic input is also narrow, allowing the coupled input to dominate receptive field sensitivity starting at distances from the receptive field center of as little as 50 μm (Figure 1D).

The coupled input also appears to be the source of the substantial variability in the shapes of H1 tuning curves. H1 receptive fields (Figure 5) range from relatively small with smooth spatial tuning curves (~80% of the total) to relatively large with irregular spatial tuning curves (~20% of the total). One source of this variability likely corresponds to differences in overall coupling strength. The small diameter but smooth receptive field (Figure 5, top curve) likely results from weak coupling whereas the larger receptive field whose tuning curve has an inflection at moderate spatial frequencies (Figure 5, second curve) likely corresponds with stronger coupling. This is consistent with our findings that the gap junction blocker, carbenoxolone, had the strongest effects on those cells that we interpreted as having stronger coupling (Figure 9), and that varying the gap junction conductance of the model produced a range of spatial tuning curves very similar to those measured in H1 cells (Figure 5).

A second source of variability in receptive field structure likely results from spatial interactions in and among dendritic trees. These interactions appear as notches and bumps in the spatial tuning curves at mid to high spatial frequencies (Figure 5, bottom two curves) that are attenuated by computationally disconnecting model gap junctions (Figure 6) and by applying carbenoxolone (Figure 8). We speculate that these irregularities result from the summation of cone signals that take a highly convoluted path through the dendritic trees of neighboring H1 cells before being coupled into the response of the recorded cell. The phases and amplitudes of these signals at the soma, where they are summed, would depend on the complex interaction of the positions of the cones and H1 cells in their disordered mosaics as well as the morphological and electrical details of the dendritic tree.

In theory, spatial interactions could also result from coupling among cones connected by telodendria (Ahnelt & Pflug, 1986; Hornstein, Verweij, & Schnapf, 2004). However, because our model did not include cone–cone coupling, the ability to reproduce irregularities at moderate spatial frequencies must be explained on other grounds. In central retina, limited cone–cone coupling has been hypothesized to reduce noise in the cone–H1 network without seriously reducing spatial resolution (DeVries et al., 2002; Hsu et al., 2000). In peripheral retina, where our measurements were made, convergence of cone signals is already so extensive that even strong cone–cone coupling would be unlikely to compromise resolution. Perhaps cone–cone coupling is responsible for irregularities sometimes seen in the H1 spatial tuning curves at high spatial frequencies, features that are not well explained by H1 cell coupling alone (Packer & Dacey, 2002). Coupling among peripheral L and M cones may also somewhat degrade color discrimination in favor of luminance discrimination (Hornstein et al., 2004).

The results we obtained using carbenoxolone would have the simplest interpretation if it could be shown that the drug effects were confined to modulating gap junction conductance. However, carbenoxolone at high doses and long application times also hyperpolarizes H1 cells and reduces their responsiveness to light, effects that are likely due to inhibition of voltage-gated calcium channels (Vessey et al., 2004). To minimize these effects, we made all of our measurements immediately after the slow depolarization in the light response was abolished but before the amplitude of the light response was substantially reduced. In any event, neither a small change in overall response amplitude nor the loss of H1-cone feedback would in and of themselves be expected to alter the receptive field structure mediated by gap junction coupling.

Implications for the nature of horizontal cell feedback

In most vertebrates, horizontal cells contribute to the formation of inhibitory surrounds (Baylor, Fuortes, & O'Bryan, 1971; Boycott & Dowling, 1969; Burkhardt, 1977; Missotten, 1965; Piccolino, 1995; Stell, 1965; Verweij et al., 2003) by providing a pathway for inhibitory lateral connections that mediate negative feedback from horizontal cells onto cones. Although the details remain controversial, negative feedback is thought to be mediated either by the inhibitory neurotransmitter gamma amino butyric acid (GABA) (reviewed by Piccolino, 1995; Wu, 1992) or by a calcium-dependent mechanism that involves gap junction hemichannels on horizontal cells and chloride currents on cone pedicles (reviewed by Kamermans & Spekreijse, 1999; Kamermans et al., 2001).

Primate H1 horizontal cell responses are most consistent with a calcium-dependent feedback mechanism. Monkey H1 horizontal cell responses (Dacey et al., 1996; Dacheux & Raviola, 1990) mimic the signature of negative feedback demonstrated in teleost horizontal cells, a slow depolarization back to the resting potential immediately following a fast hyperpolarization to stepped light onset

(Kamermans et al., 2001). As in teleost horizontal cells (Kamermans et al., 2001), this slow depolarization is blocked by both cobalt and carbenoxolone. Kamermans has argued that these drugs block calcium-dependent feedback from horizontal cells to cones. Our data are also consistent with the finding that the inhibitory surrounds of primate parasol ganglion cells are attenuated by both cobalt and carbenoxolone, but not by drugs such as picrotoxin and tetrodotoxin that disrupt GABAergic mechanisms (McMahon et al., 2004).

Differences in the effects of cobalt and carbenoxolone on the receptive fields of H1 cells also favor a calcium-dependent feedback mechanism. According to the calcium hypothesis, carbenoxolone eliminates the slow depolarization to light onset by blocking the H1 hemichannels that mediate feedback. It would also reduce response amplitude and receptive field diameter by blocking gap junctions among H1 dendrites. Low doses of cobalt, on the other hand, should interfere with calcium-dependent feedback but not affect receptive field properties mediated by cone synaptic input or gap junctions among dendrites. This prediction is consistent with our results (Figures 6–9).

Implications for ganglion cell receptive fields and color vision

If ganglion cell surrounds result from summing the receptive fields of coupled H1 horizontal cells, then H1 receptive fields must be larger than H1 dendritic trees, but smaller than ganglion cell surrounds. When we compared H1 dendritic (Wässle et al., 1989) and receptive fields (Packer & Dacey, 2002) with midget ganglion cell surrounds (Croner & Kaplan, 1995), we found that all three parameters increase in diameter from central to peripheral retina (Figure 1B). At any given eccentricity, the average H1 receptive field was larger than the average H1 dendritic tree but smaller than the average ganglion cell surround.

Although measurements in central retina are complicated by lateral shifts in ganglion cell somas away from their receptive field centers, even the most central H1 receptive fields are likely to be small enough to contribute to midget ganglion cell surrounds. Foveal H1 dendritic arbors are as small as ~16 μm in diameter (Wässle et al., 1989), slightly smaller than the 20–30 μm reported for the smallest foveal midget ganglion cell surrounds (Croner & Kaplan, 1995; Lee, Kremers, & Yeh, 1998). If the reduction in dendritic overlap with decreasing eccentricity (Wässle et al., 2000) corresponds to reduced coupling among cells, the most central H1 receptive fields will be similar in size to their dendritic fields.

By the level of the ganglion cells, the responses of the short (S), middle (M), and long (L) wavelength-sensitive cones have been reorganized into "blue/yellow" and "red/green" opponent channels. The signature of red/green spectral opponency measured in midget ganglion cells and parvocellular neurons of the lateral geniculate nucleus (De Monasterio, 1978; De Monasterio & Gouras, 1975; De Monasterio, Gouras, & Tolhurst, 1975; Derrington, Krauskopf, & Lennie, 1984; De Valois, Abramov, & Jacobs, 1966; Lankheet, Lennie, & Krauskopf, 1998; Lee et al., 1998; Martin, Lee, White, Solomon, & Ruttiger, 2001; Reid & Shapley, 1992, 2002; Wiesel & Hubel, 1966) is that stimulation of L and M cones produces responses of opposite sign.

The circuitry that implements spectral opponency remains unclear (Dacey & Packer, 2003). The "selective connection" hypothesis (Lee et al., 1998; Martin et al., 2001; Reid & Shapley, 1992, 2002; Wiesel & Hubel, 1966) proposes that cone-type-selective circuitry connects cones of one type to the receptive field center and cones of the other cone type to the receptive field surround and predicts that spectral opponency can remain strong across the retina. In contrast, the "random connection" hypothesis (Lennie, Haake, & Williams, 1991; Mullen & Kingdom, 1996; Paulus & Kröger-Paulus, 1983; Shapley & Perry, 1986) proposes that opponency results from the single cone input to the receptive field center of central midget ganglion cells. This receptive field center, which gets pure cone input by default, opposes a surround formed by horizontal cells that indiscriminately sum inputs from adjacent L and M cones. Thus, the random connection hypothesis requires no selective connections. It predicts that spectral opponency will be stronger in central retina, where the largest numbers of ganglion cell receptive field centers get inputs from single cones. In retinas with highly unequal L/M cone ratios (Roorda, Metha, Lennie, & Williams, 2001; Vimal, Pokorny, Smith, & Shevell, 1989; Wesner, Pokorny, Shevell, & Smith, 1991), opponency in central retina may get a further boost from the statistical properties of sparse sampling (Packer & Dacey, 2002). In these cases, few of the less numerous cone types are available to form an opponent surround. However, a central midget surround may get input from a single H1 cell that contacts only six or seven cones (Wässle et al., 1989). Such sparse sampling guarantees strong opponency in a few ganglion cells whose surrounds sample a homogeneous patch of cones of the type opposing the center. The remainder of the ganglion cells, whose surrounds predominantly sample cones of the same type as the center, will be weakly or nonopponent. Sparse sampling becomes effective when surround diameter is reduced below about 25 μm (Packer & Dacey, 2002), similar to the diameter of the smallest surrounds of the foveal midget cells.

Although evidence from outer retina favors the random connection hypothesis, some ganglion cell recordings are most easily explained by selective connections. All of the physiological and anatomical evidence (Dacey et al., 1996, 2000; Dacheux & Raviola, 1990; Goodchild, Chan, & Grunert, 1996; Wässle et al., 1989) shows that H1 horizontal cells get indiscriminate

input from the nearly randomly assigned (Mollon & Bowmaker, 1992; Roorda & Williams 1999; Roorda et al., 2001; Packer, Williams, & Bensinger, 1996) L and M cones in the photoreceptor mosaic above the dendritic tree. In addition, psychophysical evidence shows that spectral contrast sensitivity declines in peripheral vision (Mullen & Kingdom, 2002), consistent with the prediction of the random connection hypothesis. On the other hand, some (Lee et al., 1998; Martin et al., 2001; Reid & Shapley, 1992, 2002; Solomon et al., 2005) but not all (Diller et al., 2004) studies of ganglion cell physiology are most easily explained by ganglion cell surrounds that get pure cone inputs, results that, in light of the findings from outer retina, require the existence of cone-type-selective circuits in inner retina. Amacrine cells would be the logical candidates for mediating these selective connections. However, the existing anatomical evidence (Calkins & Sterling, 1996) suggests that such selective amacrine circuitry is unlikely. Further studies of midget ganglion cell receptive field characteristics over a range of retinal eccentricities will be required to resolve this issue.

Conclusions

Our results support the conclusion that the gradients of morphology (Wässle et al., 1989, 2000) and physiology (Packer & Dacey, 2002) of the H1 horizontal cell network result from the need for small ganglion cell receptive fields capable of mediating the high spatial resolution of the fovea. The fovea anchors a central to peripheral gradient of ganglion cell receptive field size (Croner & Kaplan, 1995). To the extent that the classical receptive field surrounds of mammalian ganglion cells are mediated by feedback from horizontal cells to cones (Mangel, 1991; McMahon et al., 2004), the existence of the fovea also explains gradients of H1 horizontal cell morphology and physiology. H1 receptive field diameter is likely determined by an interaction of dendritic arbor diameter and degree of overlap. According to this view, the small H1 receptive fields of central retina result from small dendritic trees whose minimal overlap minimizes coupling. This allows them to mediate the surrounds of central midget ganglion cells. Peripheral H1 receptive fields, on the other hand, are formed by large H1 dendritic arbors that overlap extensively, creating many opportunities for coupling to enlarge the receptive field beyond the diameter of a single dendritic tree. These receptive fields can contribute to large peripheral ganglion cell surrounds.

Acknowledgments

Supported by NIH grants EY06678, EY09625, EY01730 (Vision Research Core), RR00166 (National Primate Research Center at University of Washington), and an unrestricted grant from the Paul Kayser International Award in Retina Research (DMD). The authors thank Rob Smith for useful scientific discussions as well as for writing the modeling software and helping us with its use. We thank Vivianne Smith for helpful comments on the manuscript. We also thank Toni Haun for drawing cells and Beth Peterson for making electrodes.

Commercial relationships: none.
Corresponding author: Orin S. Packer.
Email: orin@u.washington.edu.
Address: Department of Biological Structure 357420, G514 HSC, University of Washington, Seatle WA 98195.

References

Ahnelt, P. K., & Pflug, R. (1986). Telodendrial contacts between foveolar cone pedicles in the human retina. *Experientia, 42,* 298–300. [PubMed]

Baylor, D. A., Fuortes, M. G., & O'Bryan, P. M. (1971). Receptive fields of cones in the retina of the turtle. *Journal of Physiology, 214,* 265–294. [PubMed]

Bloomfield, S. A., Xin, D., & Persky, S. E. (1995). A comparison of receptive field and tracer coupling size of horizontal cells in the rabbit retina. *Visual Neuroscience, 12,* 985–999. [PubMed]

Boycott, B. B., & Dowling, J. E. (1969). Organization of the primate retina: Light microscopy. *Philosophical Transactions of the Royal Society of London, 255B,* 109–176.

Burkhardt, D. A. (1977). Responses and receptive-field organization of cones in perch retinas. *Journal of Neurophysiology, 40,* 53–62. [PubMed]

Calkins, D. J., & Sterling, P. (1996). Absence of spectrally specific lateral inputs to midget ganglion cells in primate retina. *Nature, 381,* 613–615. [PubMed]

Croner, L. J., & Kaplan, E. (1995). Receptive fields of P and M ganglion cells across the primate retina. *Vision Research, 35,* 7–24. [PubMed]

Dacey, D. M., & Lee, B. B. (1994). The 'blue-on' opponent pathway in primate retina originates from a distinct bistratified ganglion cell type. *Nature, 367,* 731–735. [PubMed]

Dacey, D. M., Lee, B. B., Stafford, D. K., Pokorny, J., & Smith, V. C. (1996). Horizontal cells of the primate retina: Cone specificity without spectral opponency. *Science, 271,* 656–659. [PubMed]

Dacey, D. M., & Packer, O. S. (2003). Colour coding in the primate retina: Diverse cell types and cone-specific

circuitry. *Current Opinion in Neurobiology, 13,* 421–427. [PubMed]

Dacey, D. M., Packer, O. S., Diller, L., Brainard, D., Peterson, B., & Lee, B. (2000). Center surround receptive field structure of cone bipolar cells in primate retina. *Vision Research, 40,* 1801–1811. [PubMed]

Dacheux, R. F., & Raviola, E. (1990). Physiology of HI horizontal cells in the primate retina. *Proceedings of the Royal Society of London. Series B, Biological Sciences, 239,* 213–230. [PubMed]

Davidson, J. S., & Baumgarten, I. M. (1988). Glycyrrhetinic acid derivatives: A novel class of inhibitors of gap-junctional intercellular communication. Structure–activity relationships. *Journal of Pharmacology and Experimental Therapy, 246,* 1104–1107. [PubMed]

De Monasterio, F. M. (1978). Center and surround mechanisms of opponent-color X and Y ganglion cells of retina of macaques. *Journal of Neurophysiology, 41,* 1418–1434. [PubMed]

De Monasterio, F. M., & Gouras, P. (1975). Functional properties of ganglion cells of the rhesus monkey retina. *Journal of Physiology (London), 251,* 167–195. [PubMed]

De Monasterio, F. M., Gouras, P., & Tolhurst, D. J. (1975). Trichromatic colour opponency in ganglion cells of the rhesus monkey retina. *Journal of Physiology (London), 251,* 197–216. [PubMed]

Derrington, A. M., Krauskopf, J., & Lennie, P. (1984). Chromatic mechanisms in lateral geniculate nucleus of macaque. *Journal of Physiology (London), 357,* 241–265. [PubMed]

De Valois, R. L., Abramov, I., & Jacobs, G. H. (1966). Analysis of response patterns of LGN cells. *Journal of the Optical Society of America, 56,* 966–977. [PubMed]

DeVries, S. H., Qi, X., Smith, R., Makous, W., & Sterling, P. (2002). Electrical coupling between mammalian cones. *Current Biology, 12,* 1900–1907. [PubMed]

Diller, L., Packer, O. S., Verweij, J., McMahon, M. J., Williams, D. R., & Dacey, D. M. (2004). L and M cone contributions to the midget and parasol ganglion cell receptive fields of macaque monkey retina. *Journal of Neuroscience, 24,* 1079–1088. [PubMed]

Goodchild, A. K., Chan, T. L., & Grunert, U. (1996). Horizontal cell connections with short-wavelength-sensitive cones in macaque monkey retina. *Visual Neuroscience, 13,* 833–845. [PubMed]

Guan, X., Wilson, S., Schlender, K. K., & Ruch, R. J. (1996). Gap-junction disassembly and connexin 43 dephosphorylation induced by 18 beta-glycyrrhetinic acid. *Molecular Carcinogenesis, 16,* 157–164. [PubMed]

Hornstein, E. P., Verweij, J., & Schnapf, J. L. (2004). Electrical coupling between red and green cones in primate retina. *Nature Neuroscience, 7,* 745–750. [PubMed]

Hsu, A., Smith, R. G., Buchsbaum, G., & Sterling, P. (2000). Cost of cone coupling to trichromacy in primate fovea. *Journal of the Optical Society of America. A, Optics, Image Science, and Vision, 17,* 635–640. [PubMed]

Kamermans, M., Fahrenfort, I., Schultz, K., Janssen-Bienhold, U., Sjoerdsma, T., & Weiler, R. (2001). Hemichannel-mediated inhibition in the outer retina. *Science, 292,* 1178–1180. [PubMed]

Kamermans, M., & Spekreijse, H. (1999). The feedback pathway from horizontal cells to cones. A mini review with a look ahead. *Vision Research, 39,* 2449–2468. [PubMed]

Kaneko, A. (1971). Electrical connexions between horizontal cells in the dogfish retina. *Journal of Physiology, 213,* 95–105. [PubMed]

Lamb, T. D. (1976). Spatial properties of horizontal cell responses in the turtle retina. *Journal of Physiology, 263,* 239–255. [PubMed]

Lankheet, M. J., Lennie, P., & Krauskopf, J. (1998). Distinctive characteristics of subclasses of red-green P-cells in LGN of macaque. *Visual Neuroscience, 15,* 37–46. [PubMed]

Lankheet, M. J., Prickaerts, J. H., & van de Grind, W. A. (1992). Responses of cat horizontal cells to sinusoidal gratings. *Vision Research, 32,* 997–1008. [PubMed]

Lee, B. B., Kremers, J., & Yeh, T. (1998). Receptive fields of primate retinal ganglion cells studied with a novel technique. *Visual Neuroscience, 15,* 161–175. [PubMed]

Lennie, P., Haake, P. W., & Williams, D. R. (1991). The design of chromatically opponent receptive fields. In M. S. Landy & J. A. Movshon (Eds.), *Computational models of visual processing* (pp. 71–82). Cambridge: MIT Press.

Mangel, S. C. (1991). Analysis of the horizontal cell contribution to the receptive field surround of ganglion cells in the rabbit retina. *Journal of Physiology, 442,* 211–234. [PubMed]

Martin, P. R., Lee, B. B., White, A. J., Solomon, S. G., & Ruttiger, L. (2001). Chromatic sensitivity of ganglion cells in the peripheral primate retina. *Nature, 410,* 933–936. [PubMed]

McMahon, M. J., Packer, O. S., & Dacey, D. M. (2004). The classical receptive field surround of primate parasol ganglion cells is mediated primarily

by a non-GABAergic pathway. *Journal of Neuroscience, 24,* 3736–3745. [PubMed]

Mills, S. L., & Massey, S. C. (1994). Distribution and coverage of A- and B-type horizontal cells stained with Neurobiotin in the rabbit retina. *Visual Neuroscience, 11,* 549–560. [PubMed]

Missotten, L. (1965). *The ultrastructure of the human retina.* Brussels: Editions Arscia S.A.

Mollon, J. D., & Bowmaker, J. K. (1992). The spatial arrangement of cones in the primate fovea. *Nature, 360,* 677–679. [PubMed]

Mullen, K. T., & Kingdom, F. A. (1996). Losses in peripheral colour sensitivity predicted from "hit and miss" post-receptoral cone connections. *Vision Research, 36,* 1995–2000. [PubMed]

Mullen, K. T., & Kingdom, F. A. (2002). Differential distributions of red-green and blue-yellow cone opponency across the visual field. *Visual Neuroscience, 19,* 109–118. [PubMed]

Naka, K. I., & Nye, P. W. (1971). Role of horizontal cells in organization of the catfish retinal receptive field. *Journal of Neurophysiology, 34,* 785–801. [PubMed]

Naka, K. I., & Rushton, W. A. (1967). The generation and spread of S-potentials in fish (Cyprinidae). *Journal of Physiology, 192,* 437–461. [PubMed]

Naka, K. I., & Witkovsky, P. (1972). Dogfish ganglion cell discharge resulting from extrinsic polarization of the horizontal cells. *Journal of Physiology, 223,* 449–460. [PubMed]

Osborne, P. B., & Williams, J. T. (1996). Forskolin enhancement of opioid currents in rat locus coeruleus neurons. *Journal of Neurophysiology, 76,* 1559–1565. [PubMed]

Packer, O. S., & Dacey, D. M. (2002). Receptive field structure of H1 horizontal cells in macaque monkey retina. *Journal of Vision, 2,* 272–292. [PubMed]

Packer, O., Diller, L. C., Verweij, J., Lee, B. B., Pokorny, J., & Williams, D. R., et al. (2001). Characterization and use of a digital light projector for vision research. *Vision Research, 41,* 427–439. [PubMed]

Packer, O. S., Williams, D. R., & Bensinger, D. G. (1996). Photopigment transmittance imaging of the primate photoreceptor mosaic. *Journal of Neuroscience, 16,* 2251–2260. [PubMed]

Paulus, W., & Kröger-Paulus, A. (1983). A new concept of retinal colour coding. *Vision Research, 23,* 529–540. [PubMed]

Piccolino, M. (1995). Cross-talk between cones and horizontal cells through the feedback circuit. In M. B. A. Djamgoz, S. N. Archer, & S. Vallerga (Eds.), *Neurobiology and clinical aspects of the outer retina, 1st Edition* (pp. 221–248). London: Chapman & Hall.

Reid, R. C., & Shapley, R. M. (1992). Spatial structure of cone inputs to receptive fields in primate lateral geniculate nucleus. *Nature, 356,* 716–718. [PubMed]

Reid, R. C., & Shapley, R. M. (2002). Space and time maps of cone photoreceptor signals in macaque lateral geniculate nucleus. *Journal of Neuroscience, 22,* 6158–6175. [PubMed]

Roorda, A., Metha, A. B., Lennie, P., & Williams, D. R. (2001). Packing arrangement of the three cone classes in primate retina. *Vision Research, 41,* 1291–1306. [PubMed]

Roorda, A., & Williams, D. R. (1999). The arrangement of the three cone classes in the living human eye. *Nature, 397,* 520–522. [PubMed]

Shapley, R. M., Perry, V. H. (1986). Cat and monkey retinal ganglion cells and their visual functional roles. *Trends In the Neurosciences, 9,* 229–235.

Shigematsu, Y., & Yamada, M. (1988). Effects of dopamine on spatial properties of horizontal cell responses in the carp retina. *Neuroscience Research Supplement, 8,* S69–S80. [PubMed]

Smith, R. G. (1992). NeuronC: A computational language for investigating functional architecture of neural circuits. *Journal of Neuroscience Methods, 43,* 83–108. [PubMed]

Smith, R. G. (1995). Simulation of an anatomically defined local circuit: The cone-horizontal cell network in cat retina. *Visual Neuroscience, 12,* 545–561. [PubMed]

Smith, V. C., Pokorny, J., Lee, B. B., & Dacey, D. M. (2001). Primate horizontal cell dynamics: An analysis of sensitivity regulation in the outer retina. *Journal of Neurophysiology, 85,* 545–558. [PubMed]

Solomon, S. G., Lee, B. B., White, A. J., Ruttiger, L., & Martin, P. R. (2005). Chromatic organization of ganglion cell receptive fields in the peripheral retina. *Journal of Neuroscience, 25,* 4527–4539. [PubMed]

Stell, W. K. (1965). Correlation of retinal cytoarchitecture and ultrastructure in Golgi preparations. *Anatomical Record, 153,* 389–397. [PubMed]

Thoreson, W. B., & Burkhardt, D. A. (1990). Effects of synaptic blocking agents on the depolarizing responses of turtle cones evoked by surround illumination. *Visual Neuroscience, 5,* 571–583. [PubMed]

Tomita, T. (1965). Electrophysiological study of the mechanisms subserving color coding in the fish retina. *Cold Spring Harbor Symposium in Quantitative Biology, 30,* 559–566. [PubMed]

Tornqvist, K., Yang, X. L., & Dowling, J. E. (1988). Modulation of cone horizontal cell activity in the teleost fish retina. III. Effects of prolonged darkness and dopamine on electrical coupling between horizontal

cells. *Journal of Neuroscience, 8,* 2279–2288. [PubMed]

Vaney, D. I., Nelson, J. C., & Pow, D. V. (1998). Neurotransmitter coupling through gap junctions in the retina. *Journal of Neuroscience, 18,* 10594–10602. [PubMed]

Verweij, J., Hornstein, E. P., & Schnapf, J. L. (2003). Surround antagonism in macaque cone photoreceptors. *Journal of Neuroscience, 23,* 10249–10257. [PubMed]

Vessey, J. P., Lalonde, M. R., Mizan, H. A., Welch, N. C., Kelly, M. E., & Barnes, S. (2004). Carbenoxolone inhibition of voltage-gated Ca channels and synaptic transmission in the retina. *Journal of Neurophysiology, 92,* 1252–1256. [PubMed]

Vigh, J., & Witkovsky, P. (1999). Sub-millimolar cobalt selectively inhibits the receptive field surround of retinal neurons. *Visual Neuroscience, 16,* 159–168. [PubMed]

Vimal, R. L. O., Pokorny, J., Smith, V. C., & Shevell, S. K. (1989). Foveal cone thresholds. *Vision Research, 29,* 61–78. [PubMed]

Wässle, H., Boycott, B. B., & Rohrenbeck, J. (1989). Horizontal cells in the monkey retina: Cone connections and dendritic network. *European Journal of Neuroscience, 1,* 421–435. [PubMed]

Wässle, H., Dacey, D. M., Haun, T., Haverkamp, S., Grunert, U., & Boycott, B. B. (2000). The mosaic of horizontal cells in the macaque monkey retina: With a comment on biplexiform ganglion cells. *Visual Neuroscience, 17,* 591–608. [PubMed]

Weiler, R., Pottek, M., He, S., & Vaney, D. I. (2000). Modulation of coupling between retinal horizontal cells by retinoic acid and endogenous dopamine. *Brain Research Reviews, 32,* 121–129. [PubMed]

Wesner, M. F., Pokorny, J., Shevell, S. K., & Smith, V. C. (1991). Foveal cone detection statistics in color-normals and dichromats. *Vision Research, 31,* 1021–1037. [PubMed]

Wiesel, T. N., & Hubel, D. H. (1966). Spatial and chromatic interactions in the lateral geniculate body of the rhesus monkey. *Journal of Neurophysiology, 29,* 1115–1156. [PubMed]

Witkovsky, P., Owen, W. G., & Woodworth, M. (1983). Gap junctions among the perikarya, dendrites, and axon terminals of the luminosity-type horizontal cell of the turtle retina. *Journal of Comparative Neurology, 216,* 359–368. [PubMed]

Wu, S. M. (1992). Feedback connections and operation of the outer plexiform layer of the retina. *Current Opinion in Neurobiology, 2,* 462–468.

Yamada, E., & Ishikawa, T. (1965). The fine structure of the horizontal cells in some vertebrate retinae. *Cold Spring Harbor Symposium on Quantitative Biology, 30,* 383–392. [PubMed]